



General palaeontology, systematics and evolution

A new basilosaurid (Cetacea, Pelagiceti) from the Late Eocene to Early Oligocene Otuma Formation of Peru

Un nouvel archéocète basilosauridé (Cetacea, Pelagiceti) de la Formation Otuma (Éocène supérieur) du Pérou

Manuel Martínez-Cáceres*, Christian de Muizon

Muséum national d'histoire naturelle, UMR 7207, Centre de recherche sur la paléobiodiversité et les paléoenvironnements, MNHN, CNRS, UPMC, 57, rue Cuvier, CP 38, 75231 Paris cedex 05, France

ARTICLE INFO

Article history:

Received 1st December 2010

Accepted after revision 6 March 2011

Available online 2 May 2011

Presented by Philippe Taquet

Keywords:

Cetacea

Archaeocete

Basilosauridae

Late Eocene-Early Oligocene

Peru

Mots clés :

Cetacea

Archéocète

Basilosauridae

Éocène supérieur-Oligocène inférieur

Pérou

ABSTRACT

Cynthiacetus peruvianus nov. sp. is a new basilosaurid species, from Late Eocene to Early Oligocene Otuma Formation of Peru. It is the first described archaeocete in South-America and is represented by a sub-complete skeleton. *C. peruvianus* differs from *C. maxwelli* (middle to Late Eocene of Egypt and United States) principally in having one cuspid less on both mesial and distal sides of p3 and p4. *Cynthiacetus* is among the largest basilosaurids. Its more characteristic features are located on its postcranial skeleton: large vertebral foramina on cervical vertebrae and absence of ventral expansion of the transverse process on C3–C5. Besides, *C. peruvianus* presents the greatest number of thoracic vertebrae (20) and ribs observed in Cetacea and the first thoracics have an almost vertical neural spine. A preliminary parsimony analysis establishes the monophyly of the Basilosauridae on the basis of three unambiguous cranial synapomorphies. However, within the Basilosauridae, the most diagnostic characters are observed on the postcranial skeleton.

© 2011 Académie des sciences. Published by Elsevier Masson SAS. All rights reserved.

RÉSUMÉ

Cynthiacetus peruvianus nov. sp. est une nouvelle espèce de basilosauridé, provenant de la Formation Otuma de l'Éocène supérieur-Oligocène inférieur du Pérou. Il s'agit du premier archéocète décrit en Amérique du Sud et représenté par un squelette subcomplet. *Cynthiacetus peruvianus* se différencie de *C. maxwelli* (de l'Éocène moyen et supérieur de l'Égypte et des États-Unis) par la présence d'une cuspid en moins sur les bords mésial et distal de p3 et p4. *Cynthiacetus* est parmi les plus grands basilosauridés. Ses caractères les plus discriminants se situent sur son squelette postcrânien : présence de grands foramina vertébro-artériels dans les vertèbres cervicales et absence des expansions ventrales des processus transverses de C3–C5. De plus, *C. peruvianus* présente le plus grand nombre de vertèbres thoraciques (20) et de côtes observées chez les Cetacea et l'épine neurale est presque verticale dans les premières thoraciques. Une analyse de parcimonie préliminaire établit la monophylie des Basilosauridae sur la base de trois synapomorphies crâniennes non ambiguës. Cependant, au sein des Basilosauridae, les caractères les plus diagnostiques sont observés au niveau du squelette postcrânien.

© 2011 Académie des sciences. Publié par Elsevier Masson SAS. Tous droits réservés.

* Corresponding author.

E-mail address: mcaceres@mnhn.fr (M. Martínez-Cáceres).

1. Introduction

The paraphyletic Archeoceti is the stem group of the Neoceti (modern cetaceans: toothed and baleen whales), which is regarded as monophyletic by Fordyce and Muizon (2001). Among archaeocetes, the most derived taxa are included in the family Basilosauridae (Barnes and Mitchell, 1978; Uhen, 1998) regarded as paraphyletic (Uhen, 2004; Uhen and Gingerich, 2001). Basilosaurids have been reported from the Tethys Sea and from both North Atlantic and South Pacific Oceans (Fordyce, 1985; Gingerich, 1992, 2007, 2010; Gingerich and Uhen, 1996; Gingerich et al., 1997; Kellogg, 1936; Köhler and Fordyce, 1997; Uhen, 1998, 2004, 2005; Uhen and Gingerich, 2001).

Marocco and Muizon (1988), Fordyce and Muizon (2001), and Uhen et al. (2008) have pointed out the presence of archaeocetes in the Pacific Coast of South-America, but no specimen has been described yet. In 1977, one of the authors (C.M.) collected an almost complete basilosaurid skeleton in the Late Eocene to Early Oligocene Otuma Formation of Peru (described by DeVries, 1998). This specimen is the first archeocete described from South-America and is referred to a new taxon. A preliminary description and parsimony analysis are presented here. Because of its remarkable completeness and preservation, this specimen is critical to the understanding of cetacean evolution and modern cetaceans' emergence.

2. Materials and methods

In the following description, the taxa Protocetidae, Basilosauridae and Dorudontinae are referred to, although they have been regarded as paraphyletic (Geisler and Sanders, 2003; Uhen, 2004; Uhen and Gingerich, 2001). Protocetidae include the most derived non-Pelagiceti (Basilosauridae + Neoceti) cetaceans; Basilosauridae includes all Pelagiceti except Neoceti; and Dorudontinae refers to the artificial assemblage of basilosaurids lacking the anteroposterior elongation of the centrum in posterior thoracic, lumbar and anterior caudal vertebrae. This latter feature is only observed in Basilosaurinae Cope 1868 (*Basilosaurus* and *Basiloterus*).

A phylogenetic analysis was carried out using a matrix of 31 characters. Characters were selected from Uhen and Gingerich (2001), Geisler et al. (2005) and other cranial and postcranial new characters (Supplementary data). Sixteen taxa have been coded: Pakicetidae, Ambulocetidae, Remingtonocetidae, three protocetids (*Rodhocetus atavus*, *Maiacetus innus* and *Georgiacetus vogtlensis*), eight basilosaurids (*Basilosaurus isis*, *Dorudon atrox*, *Zygorhiza kochii*, *Saghacetus osiris*, *Cynthiacetus maxwelli*, *C. peruvianus*, *Ancalacetus simonsi* and *Chrysocetus healyorum*), one Mysticeti (ChM PV5720) and one Odontoceti (*Simocetus rayii*). The program used for the phylogenetic analysis is TNT version 1.1 (Goloboff et al., 2003).

Institutional abbreviations: MMNS Mississippi Museum of Natural Science, Jackson, Mississippi, USA; MNHN Muséum national d'histoire naturelle, Paris, France; ChM The Charleston Museum, Charleston, South Carolina, USA; USNM United States National Museum of Natural History, Smithsonian Institution, Washington DC, USA.

Anatomical abbreviations (For Figs. 3 and 4): **aoc**, anterior (ventral) orbital crest; **apf**, antorbital process of the frontal; **app**, anterior process of the periotic; **BO**, basioccipital; **BS**, basisphenoid; **ch**, cranial hiatus; **cf**, external carotid foramen; **eam**, external auditory meatus; **EO**, exoccipital; **fb**, falcate process of the basioccipital; **fc**, fenestra cochlea; **fe**, falcate process of the exoccipital; **fo**, foramen pseudoovale; **Fr**, frontal; **fs**, falciform process of the squamosal; **fv**, fenestra vestibuli; **gl**, glenoid fossa; **gtt**, groove for the tensor tympani muscle; **J**, jugal; **La**, lacrymal; **lpt**, lateral lamina of the pterygoid; **Max**, maxilla; **mf**, fossa for malleus; **mpt**, medial lamina of the pterygoid; **nc**, nuchal crest; **nf**, nutrient foramina for the innervation and vascularisation of the eye musculature; **oc**, occipital condyle; **opc**, optical canal; **Orb**, orbitosphenoid; **Pa**, parietal; **PE**, periotic; **pgp**, postglenoid process of the squamosal; **poc**, posterior orbital crest; **ppe**, paroccipital process of exoccipital; **ppf**, postorbital process of the frontal; **ppp**, posterior process of the periotic; **pr**, promontorium; **PT**, pterygoid; **pts**, pterygoid sinus; **sgc**, squamosal contact for the sigmoid process of the tympanic; **sph.f**, sphenopalatine foramen; **SO**, supraoccipital; **sopf**, supraorbital process of the frontal; **SQ**, squamosal; **V**, vomer; **VII**, foramen for the facial nerve (cranial nerve VII); **zyg**, zygomatic process of the squamosal.

3. Systematic palaeontology

Cetacea Brisson 1762

Pelagiceti Uhen 2008

Basilosauridae Cope 1867

Included genera: *Ancalacetus*, *Basilosaurus*, *Basiloterus*, *Chrysocetus*, *Cynthiacetus*, *Dorudon*, *Masracetus*, *Saghacetus*, *Stromerius*, *Zygorhiza*.

Cynthiacetus Uhen 2005

Type species: *Cynthiacetus maxwelli* Uhen 2005.

Emended diagnosis. Large basilosaurid lacking vertebral elongation observed in *Basilosaurus*; skull slightly shorter than *Basilosaurus* and significantly longer than all other dorudontines (e.g., *Dorudon*, *Zygorhiza*, *Saghacetus*). *Cynthiacetus* differs from all other basilosaurids in: nasal strongly tapering anteriorly in both species (even more than in *Dorudon*); atlas with a high, massive and dome-shaped neural arch; vertebral foramina on the cervical vertebrae significantly larger; absence of the ventral expansion of the transverse processes in cervical vertebrae. The supraoccipital shield of *Cynthiacetus* proportionally wider than that in *Saghacetus*; nuchal crest posterodorsally oriented (anterodorsally in *Zygorhiza*).

Cynthiacetus peruvianus, nov. sp.

Etymology. From Peru, the country where the holotype was found.

Holotype. MNHN.F.PRU 10 (Fig. 1), an almost complete skeleton of a young adult specimen including: skull, dentaries, upper and lower dentitions, petro-tympanic, hyoid, sub-complete right forelimb, partial right hindlimb, cervical, thoracic, lumbar, anterior caudal vertebrae, and ribs.

Type Locality. Paracas Bay, at about the level of the Km 240 of the South Panamerican Highway. The

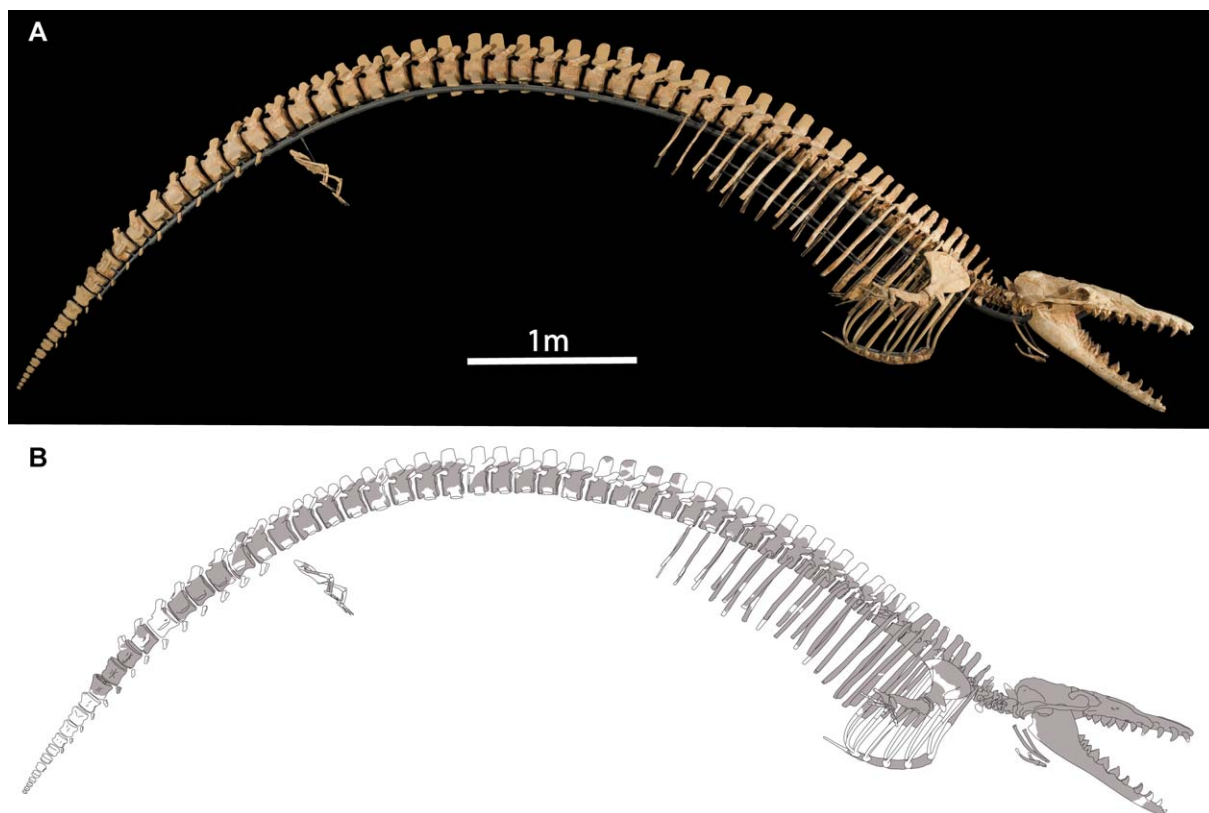


Fig. 1. *Cynthiacetus peruvianus* nov. sp. (holotype MNHN.F.PRU 10). A) Right lateral view of the skeleton. B) Grey-shaded regions indicate the preserved parts of the holotype.

Fig. 1. *Cynthiacetus peruvianus* nov. sp. (holotype MNHN.F.PRU 10). A) Vue latérale droite du squelette. B) L'ombrage grisé indique les parties conservées de l'holotype.

holotype was found approximately 2.5 km to the north-east to the type-section of the Otuma Formation (S 13°52'54.3"; W 76°14'13.4").

Type Formation. Otuma Formation, described by DeVries (1998), DeVries et al. (2006) and Uhen et al. (2008) provided a Late Eocene age (38–36Ma) based on the microfossil correlations and Ar/Ar isotopes dating at base of the formation. An Early Oligocene age of 33 Ma is provided for the top of the Formation (DeVries, 1998; DeVries et al., 2006). The age of *C. peruvianus* therefore spans from 38 Ma to 33 Ma.

Diagnosis. *C. peruvianus* differs from *C. maxwelli* in having one cuspid less on both mesial and distal edges on p3 and p4; anteroposteriorly shorter and higher dome-shaped neural arch on the atlas; proximo-distally longer and anteroposteriorly more slender humerus, radius and ulna. *Cynthiacetus peruvianus* presents the largest number of thoracic vertebrae (20) and ribs observed in all known cetaceans. Besides, the spinal processes of anterior thoracic vertebrae are more vertical than in *Basilosaurus*, *Dorudon* and *Saghacetus*. However, because these two characters are not preserved in *C. maxwelli*, they may very well represent generic characters for *Cynthiacetus*.

3.1. Description

3.1.1. Skull

The skull of MNHN.F.PRU 10 (Fig. 2ABCD) closely resembles that of other basilosaurids. Its length approaches that of *Basilosaurus* and is approximately 40% longer than that of *Dorudon* or *Zygorhiza* and 60% longer than that of *Saghacetus*. Cranial measurements are accessible in the [Supplementary data](#). The anterior portion of the rostrum is twisted to the left, a condition which is probably pathologic but clearly emphasized by a distortion due to fossilisation. The anterior 40% of the rostrum is formed by the premaxillae and the vomer. The dorsomedial edges of the premaxillae do not contact at the midline and form the roof of the mesorostral groove as far back as the canine, on approximately half of the length of the rostrum. Anterolaterally, the PMx-Mx suture is oblique and extends posteriorly from the ventrolateral border of the rostrum, behind the embrasure pit for c1 to the lateral edge of the nasal, at approximately the level of the P3–4 boundary. The premaxilla articulates posteriorly with the anterior 60% length of the lateral edge of the nasal. The ascending process of the maxilla contacts medioposteriorly the nasal but does not reach the posterior apex of

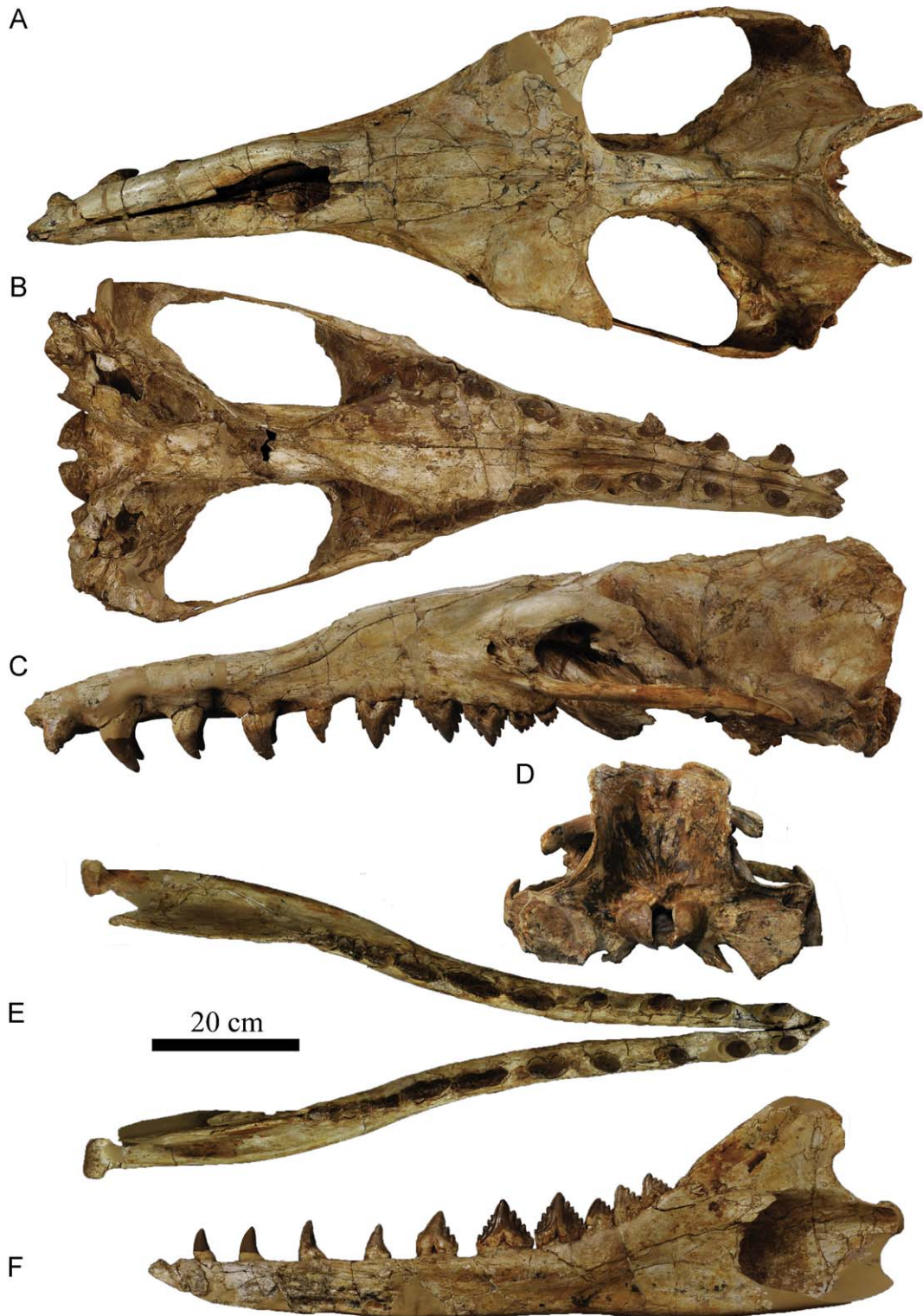


Fig. 2. *Cynthiacetus peruvianus* nov. sp. (holotype MNHN.F.PRU 10). Skull in A) dorsal; B) ventral; C) lateral; D) occipital views; E) mandible in occlusal view; F) right dentary in medial view.

Fig. 2. *Cynthiacetus peruvianus* nov. sp. (holotype MNHN.F.PRU 10). Crâne en vue A) dorsale ; B) ventrale ; C) latérale ; D) occipitale ; E) mandibule en vue occlusale ; F) dentaire droit en vue médiale.

the nasal, which articulates with the frontal, a condition also observed in *D. atrox* and *B. isis*. In *S. osiris* and in one specimen of *Z. kochii* (USNM 11962), the posterior edge of the maxilla is posterior to the posterior edge of the nasal and contacts medially the frontal. The nasal strongly tapers anteriorly and has its greatest width at the level of the triple point Mx-PMx-Na. As *D. atrox* and *B. isis*, both species of *Cynthiacetus* have an lanceolate-shaped nasal, while *S. osiris* and *Z. kochii* (except for USNM11962) present an oval nasal with the lateral edges of both nasals being roughly parallel to the midline. The posterior apices of the nasals diverge and are separated by an anterior projection of the frontals. This feature is accentuated in *D. atrox* and *B. isis* and absent in *S. osiris*, where the nasals are in contact at their posterior apices. While some specimens of *Z. kochii* (e.g. USNM 11962, USNM 16638) present a short anterior process of the frontals wedged between the posterior edges of the nasals, some other specimens lack this feature (USNM 16639, MMNS VP130). Therefore, this condition is probably variable among basilosaurids.

The infraorbital foramen is located above the posterior edge of P2. The anterior edge of the nasals is missing but it is possible to evaluate that it reached the level of the anterior edge of P2. Lacrymal and jugal are unfused and form respectively the anterior and the ventral edges of the orbit. As in *Dorudon*, the lacrymal presents three conspicuous grooves posterior to the lacrymal canal. The large and sub-triangular supraorbital process of the frontal overhangs the orbit (Fig. 3). Its ventral side forms the roof of the orbit and presents a deeply concave and medially oriented triangular cavity bordered by both ventral (anterior) and dorsal (posterior) optic crests. Between the optic crests opens the optic foramen, laterally facing. Posteroventral to the optic foramen is the orbital fissure through which the ophthalmic nerve (V1) reaches the orbital region. Anterior to the ventral orbital crest is a large sphenopalatine foramen, bounded by the frontal, the maxillary and the palatine. This foramen transmits the caudal nasal nerve which is part of the maxillary branch of the trigeminal nerve (V2). As in *Dorudon*, there is a large maxillary foramen (i.e. the posterior foramen of the infraorbital canal) in the anterior wall of the orbit. The maxillary foramen is formed dorsally by the frontal, medially and ventrally by the maxilla and laterally by the lacrymal. It conducts the infraorbital nerve, which is also part of the maxillary branch of the trigeminal nerve (V2).

The palate is very narrow anteriorly (mostly formed by the ventral surface of the premaxilla) and greatly widens posteriorly from P1 to M2 (mostly formed by the ventral surface of the maxilla). From the anterior edge of the canine, the premaxillae are wedged posteriorly between the maxillae until the level of P2. The palate bears deep embrasure pits, which receive the corresponding lower tooth. On the premaxilla, they are lateral to the tooth row and progressively move medially in the maxilla. Posterior to P4 the palate narrows and has a triangular morphology, with a pointed extremity, which extends well posteriorly to M2, at about the anterior third of the temporal fossa. This triangular region is formed by the horizontal part of the palatines, which have a bell-shaped suture with the maxillae. A small palatine foramen is located roughly in the

middle of each palatine. Laterally, the vertical portion of the palatine participates to the medial wall of the orbital region. The palatine articulates posteriorly with the pterygoid.

The Fr-Pa suture is anterolaterally oriented from the midline to the lateral border of the intertemporal constriction. At the level of the postorbital process it turns posteroventrally on 3 cm and then turns anteroventrally to form a long anteriorly convex suture on half of the height of the lateral wall of the skull. At this point, the anterior edge of the parietal forms a posteroventrally-oriented suture with the alisphenoid, which reaches the anterior edge of the squamosal, anterodorsal to the subtemporal crest. Anteriorly, the alisphenoid forms the ventrolateral wall of the braincase, while parietal forms its dorsolateral wall. From the anterior border of the subtemporal crest, the Pa-Sq suture runs posterodorsally and then turns posteroventrally at about the level of the mid-height of the supraoccipital. Here, it reaches the nuchal crest roughly at the level of the supraoccipital-exoccipital suture. The intertemporal constriction is much longer than in neocetes and the sagittal crest reaches the vertex of the skull posteriorly. The parietal exhibits a large foramen and the parasagittal crest is hardly present as a slight inflation of the lateral edge of the intertemporal constriction. From the vertex, on each side of the skull, the parietals and the supraoccipital form the nuchal crest, which is posterodorsally oriented as in *Basilosaurus* or *Dorudon*. Ventrally, the nuchal crest is formed by both squamosal and exoccipital. The transverse constriction of the nuchal crest is less pronounced than in *Saghatetus* and protocetids. The wings of the supraoccipital shield strongly project posterodorsally. In the dorsomedial region of the supraoccipital shield are two prominent tuberosities for attachment of the nuchal ligament.

The pterygoid articulates anteriorly with the palatine (Fig. 4). Both left and right pterygoids are incomplete but the right is better preserved. Anteriorly, the pterygoid forms the lateral edges of the choanae, while posteriorly it splits into lateral and medial lamina and forms a deep sinus. The lateral lamina articulates with the alisphenoid, forms the lateral wall of the pterygoid sinus and contacts the squamosal anterior to the falciform process and to the foramen pseudovalve (passage for the mandibular branch of the trigeminal nerve, V3). The medial lamina forms the medial wall of the large pterygoid sinus; it contacts the anterior border of the falcate process of the basioccipital and covers part of the vomer, which in turn covers the basisphenoid. The roof and the dorsolateral wall of the pterygoid sinus are formed partially by the alisphenoid and the squamosal. Posterolateral to the falciform process is a wide and flat glenoid fossa. The zygomatic process of the squamosal is transversely thin with a distinctly convex dorsal edge. It strongly tapers anteriorly. The postglenoid process is incomplete in both sides. It is much wider than longer, with a straight vertical anterior face and a posteriorly convex posterior face.

The basisphenoid-basioccipital suture is fused but distinctly thickened. The massive falcate process of the basioccipital extends ventrolaterally. The exoccipital participates to the falcate process (Fig. 4). Posterior to the

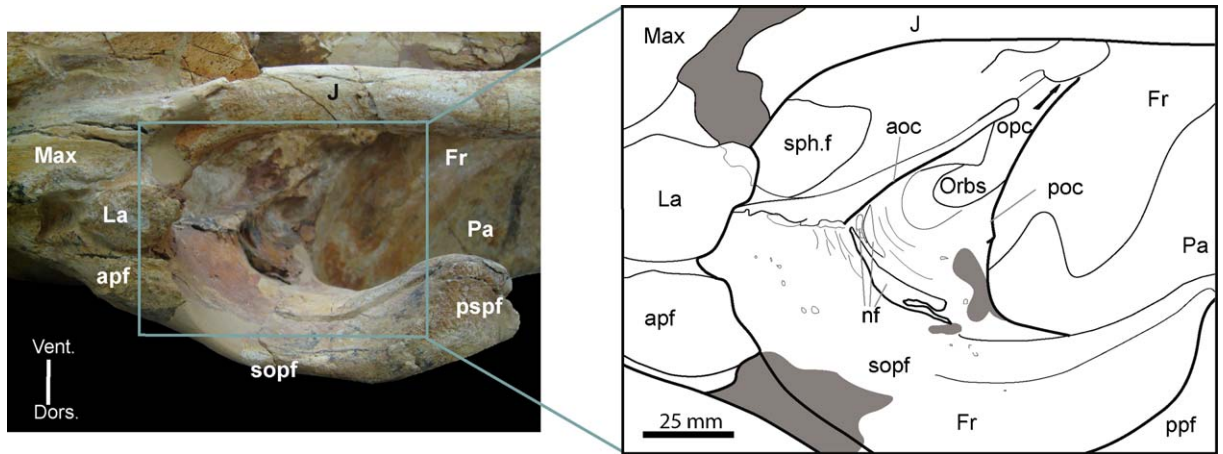


Fig. 3. Orbital region of *Cynthiacetus peruvianus* nov. sp (holotype MNHN.F.PRU 10). Ventrolateral view. (Abbreviations, see section 2).

Fig. 3. Région orbitaire de *Cynthiacetus peruvianus* nov. sp (holotype MNHN.F.PRU 10). Vue ventro-latérale. (Abréviations, voir section 2).

pterygoid sinus, the posterior lacerate foramen is bordered by the squamosal and the basioccipital. Posterior to the posterior lacerate foramen is the large cranial hiatus.

The periotic is tightly articulated to the skull. The short anterior process and the lateral face of the tegmen tympani articulate laterally with the medial side of the falciform process of the squamosal, while the elongate posterior process separates the external auditory meatus from the paraoccipital process of the exoccipital (Fig. 4). As in other dorudontines, the anterior process of MNHN.F.PRU 10 is elliptical in longitudinal cross-section and its apex turns

medially. The pars cochlearis is well preserved on the right side and its anteromedial corner lacks the anteriorly oriented bump-like protuberance observed in *Dorudon* (Uhen, 2004). Both tympanic bullae are preserved and virtually complete. The sigmoid process contacts the squamosal while its broken anterior pedicle should contact the pars cochlearis. The dorsal face of the involucrum (posterior and medial portion) and the lateral lip contact respectively the falcate process (formed by the both basioccipital and exoccipital) and the falciform process of the squamosal. The involucrum is shorter than in modern cetaceans.

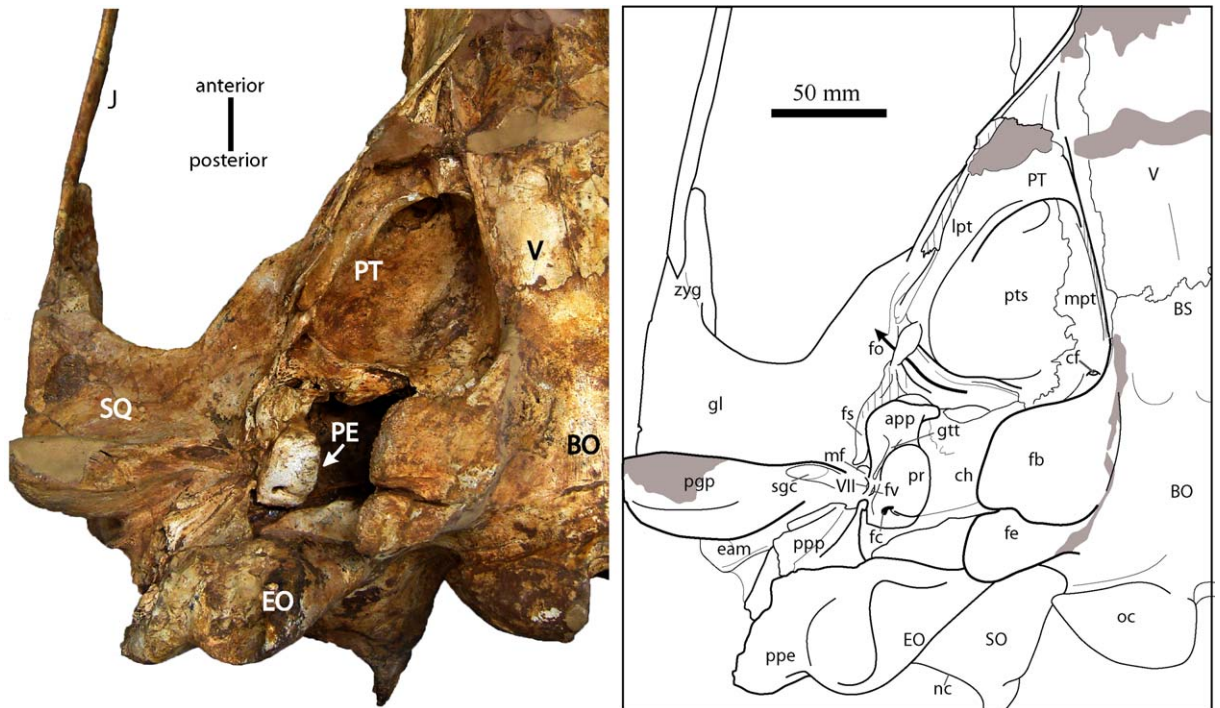


Fig. 4. Basicranium of *Cynthiacetus peruvianus* nov. sp. (holotype MNHN.F.PRU 10). Ventral view. (Abbreviations, see section 2).

Fig. 4. Basicranium de *Cynthiacetus peruvianus* nov. sp. (holotype MNHN.F.PRU 10). Vue ventrale. (Abréviations, voir section 2).

3.1.2. Mandible

Dentaries of MNHN.F.PRU 10 are virtually complete (Fig. 2EF). The dentary also presents the torsion observed in the rostrum and the anterior portion of both dentaries is slightly shifted to the left. However, the torsion in the dentaries is much less pronounced than in the skull. The symphysis is unfused and extends posteriorly until the level of the P2. As in other basilosaurids, numerous foramina pierce dentaries in lateral view. The coronoid process is more elevated than in neocetes and bears a small crest in its lateral surface, near the dorsal margin. On the medial view, the mandibular foramen or fossa is large and oval.

3.1.3. Dentition

C. peruvianus presents the typical dental formula observed in basilosaurids: (3I/3i; 1C/1c; 4P/4p; 2M/3m). The crowns of i1s and right i2–3 are missing. The left i2 is incomplete. All the other teeth are complete. Incisors and canines are conical and single-rooted. The canine is the biggest caniniform tooth in the upper and lower dentition and i1 the smallest. As in *Dorudon*, incisors and canines have well-developed mesial and distal carinae and strongly wrinkled enamel. Measurements are given in supplementary information.

All premolars are double-rooted and compressed transversely. Except for p1, all premolars bear accessory denticles on mesial and/or distal margins (Supplementary data). Compared to *C. maxwelli*, *C. peruvianus* possesses one less accessory denticle in both mesial and distal sides on p3 and p4. Molars are double-rooted teeth and are significantly smaller than premolars. The anterior root on the inferior molars presents a long sulcus on its mesial side which represents the fusion of both anterior roots. As in *C. maxwelli* and other basilosaurids, the posterior root of P3–M1 expands lingually. This is the result of the fusion of both posterior roots of the teeth. Upper molars present accessory denticles on both mesial and distal sides, while lower molars only bear accessory denticles on the distal side. Besides, lower molars present a distinct crest on their mesiolingual face as observed in other basilosaurids.

3.1.4. Axial skeleton

Cervical vertebrae. The cervical vertebrae are unfused. Their anteroposterior compression is similar to that of other basilosaurids. It is more pronounced than in protocetids and less than in modern cetaceans. In general aspect, the cervical vertebrae of MNHN.F.PRU 10 are similar to those of the holotype of *C. maxwelli*. The atlas differs from that of other basilosaurids except *C. maxwelli*, in having a high, massive and dome-shaped neural arch (Fig. 5). However, the neural arch is shorter and higher in *C. peruvianus* than in *C. maxwelli*. Besides, in *Cynhiacetes* the anterior lamina of the transverse processes is dorsally oriented, while in other dorudontines this lamina is anterodorsally oriented. The neural spine of the axis is incomplete in MNHN.F.PRU 10 but its base is transversally narrow and anteroposteriorly longer than in other dorudontines. This feature is not observable in *C. maxwelli*, where the axis is seriously damaged. As in *Saghacetus*, the C3–C7 of *Cynhiacetes* bear a vertebrarterial foramen larger than in other basilosaurids and lack the ventral expansion of the trans-

verse processes in C3–C5 visible in most other basilosaurids (e.g. *Dorudon atrox* in Fig. 5). Measurements are given in Supplementary data.

Thoracic vertebrae. A complete series of twenty thoracic vertebrae, twenty pairs of ribs and five sternal elements are preserved in MNHN.F.PRU 10. *Cynhiacetes peruvianus* is the cetacean with the highest number of thoracics. Unlike other basilosaurids, the spinal process in first thoracic is almost vertical, while in *Saghacetus* or *Basilosaurus* it is strongly tilted backwards. The first ten thoracics have two costal foveae and are slightly larger than cervical vertebrae. The fourteen thoracic (T14) is the first thoracic to possess a single costal fovea. From T8, the width and height of the centra increase considerably. As a result, the centrum of T20 is almost twice bigger than that of T1. The transverse processes are laterally oriented in most thoracics and lateroventrally oriented in the last three thoracics.

Lumbar vertebrae. Sixteen vertebrae are preserved in the lumbar region. Unlike *Basilosaurus*, the centra of posterior thoracics and lumbar are not significantly elongated (Supplementary data). The proportions are similar to those of *Dorudon* and other dorudontines (Kellogg, 1936; Gingerich and Uhen, 1996; Uhen, 2004, 2005). As in all other basilosaurids, no sacral region is differentiated.

Caudal vertebrae. Ten caudal vertebrae and one chevron are preserved in MNHN.F.PRU 10. They belong to the anterior section and are similar in morphology than those of *Dorudon*. From the Ca5, the transverse process is perforated by a single foramen.

3.1.5. Forelimb

Only the right forelimb is preserved in MNHN.F.PRU 10. It is near complete and includes the scapula, humerus, radius, ulna, five carpals, four partial metacarpals and two partial phalanges (Fig. 6). In general morphology, the forelimb of *Cynhiacetes* is similar to that of the other known basilosaurids except *Ancalacetus* which possesses a particular architecture among basilosaurids (Gingerich and Uhen, 1996). The scapula is triangular and the infraspinous fossa is considerably larger than the supraspinous fossa. The anterior border (partially reconstructed) was probably convex as is observed in *Dorudon*.

As all other basilosaurids, the humerus bears a prominent deltopectoral crest which is anteriorly oriented and occupies most of the shaft. The humerus contacts the radius and the ulna by a single articular trochlea. The morphology of the trochlea only allows flexion and extension of the arm inhibiting pronation and supination movements. Both radius and ulna are transversally flattened. Proportionally, the forelimb of *Cynhiacetes* is slightly smaller than that of *Basilosaurus* or *Dorudon* but considerably larger than that of *Ancalacetus*. The holotype of *C. maxwelli* (MMNS VP 445) possesses a brachium (humerus) and an antebrachium (ulna and radius) proximo-distally shorter and anteroposteriorly larger than MNHN.F.PRU 10. Unlike *Ancalacetus*, except for the magnum-trapezoid bone, there is no carpal fusion. This condition is also observed in *Dorudon*.

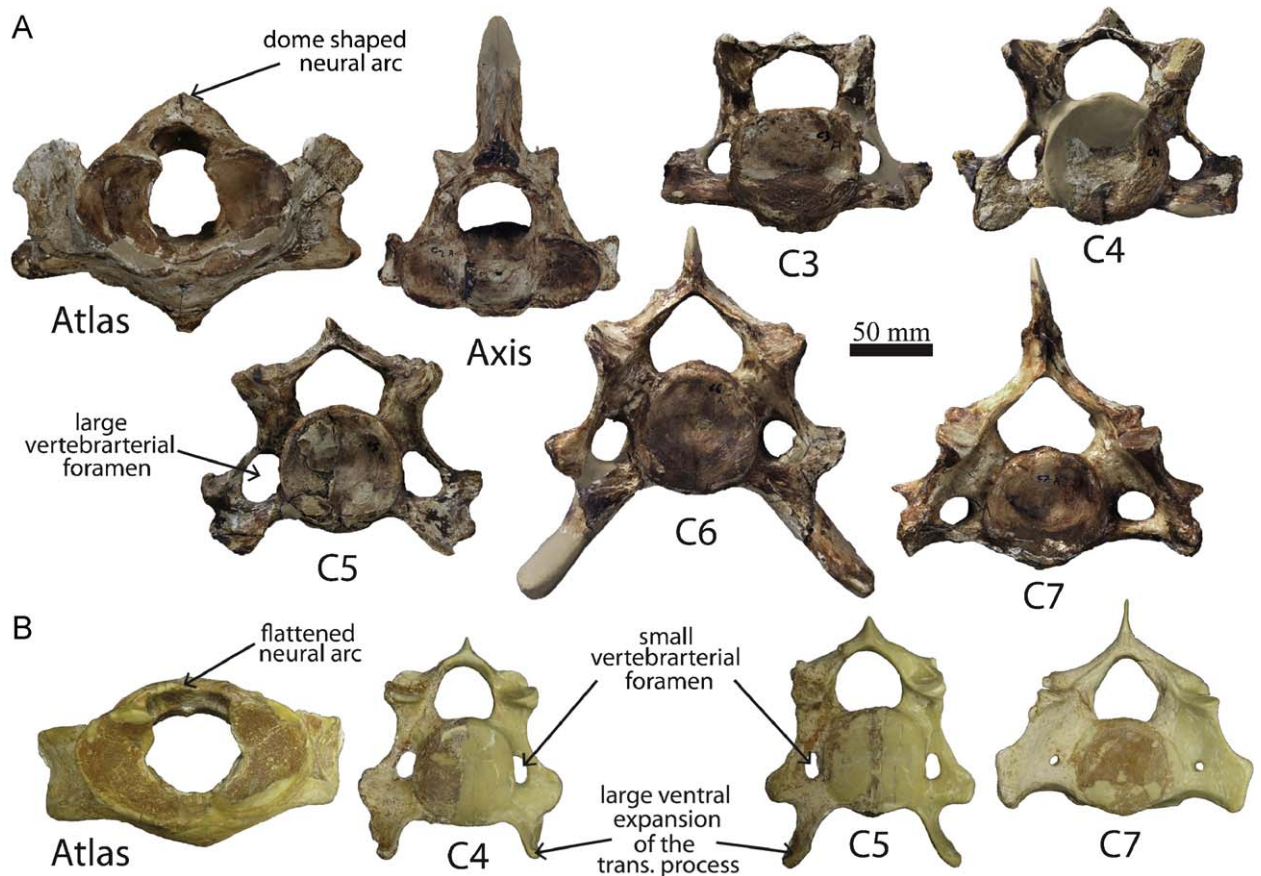


Fig. 5. Anterior view of the cervical vertebra of A) *Cynthiacetus peruvianus* nov. sp. (holotype MNHN.F.PRU 10) and B) *Dorudon atrox* UM 101222.
Fig. 5. Vue antérieure des vertèbres cervicales de A) *Cynthiacetus peruvianus* nov. sp. (holotype MNHN.F.PRU 10) et B) *Dorudon atrox* UM 101222.

3.1.6. Hindlimb

The left and most of the right hindlimb are missing. Only a non-diagnostic fragment of the innominate and incomplete femur, tibia, fibula and three first phalanges are preserved. The hindlimb seems to be quite similar in general morphology to that of *Basilosaurus* (Gingerich et al., 1990) but considerably smaller. The proximal portion of the femoral diaphysis is anteroposteriorly compressed while the rest of the diaphysis is tubular. Unlike *Basilosaurus*, there is no fusion between both epiphysis of the tibia and the fibula in MNHN.F.PRU 10, but this condition is probably related to the ontogenetic stage of the specimen (young adult).

4. Phylogeny and discussion

One most parsimonious tree of 83 steps (RI = 0.825) was obtained using TNT 1.1, Branch and Bound research (search by implicit enumeration option) (Fig. 7). Data matrix and character list are given in [supplementary data](#). Basilosauridae appears to be monophyletic and sister taxon of Neoceti. This relationship is also obtained by Luo and Gingerich (1999) and Fitzgerald (2009). Moreover, in agreement with Geisler and Sanders (2003) and Uhen (2004), Protocetidae are paraphyletic. Basilosauridae are supported by three

non-ambiguous synapomorphies: palate narrows at the level of P4 (character 4); supraorbital process width more than 1.4 the width of the base of the rostrum, at the level of the anteorbital notch (character 7); and anterior edge of the orbit at the level of P4 or P4/M1 (character 9).

The result differs from Uhen (2004) where Basilosauridae are paraphyletic. The genus *Cynthiacetus* is monophyletic and supported by three non-ambiguous synapomorphies: large vertebrarterial foramina in the cervical region (character 25); reduced ventral extension of the transverse processes in C3–C5 (character 24); and high and dome-shaped neural arc in the atlas (character 22).

D. atrox and *B. isis* form a clade which is the sister taxa of *Cynthiacetus*. They share a well-developed anterior process of the frontal, which separates both medial edges of frontals posteriorly (character 5, state 2). The clade formed by *Cynthiacetus*, *D. atrox* and *B. isis* has one unambiguous synapomorphy: nasals tapers anteriorly, with the anterior half of lateral edge of the nasal being anteromedially oblique (character 6).

Neoceti and Pelagiceti appear as monophyletic. At the base within Basilosauridae is a clade formed by *Zygorhiza* and *Chrysoctetus*. This result is different from previous studies, where Basilosauridae were found paraphyletic and

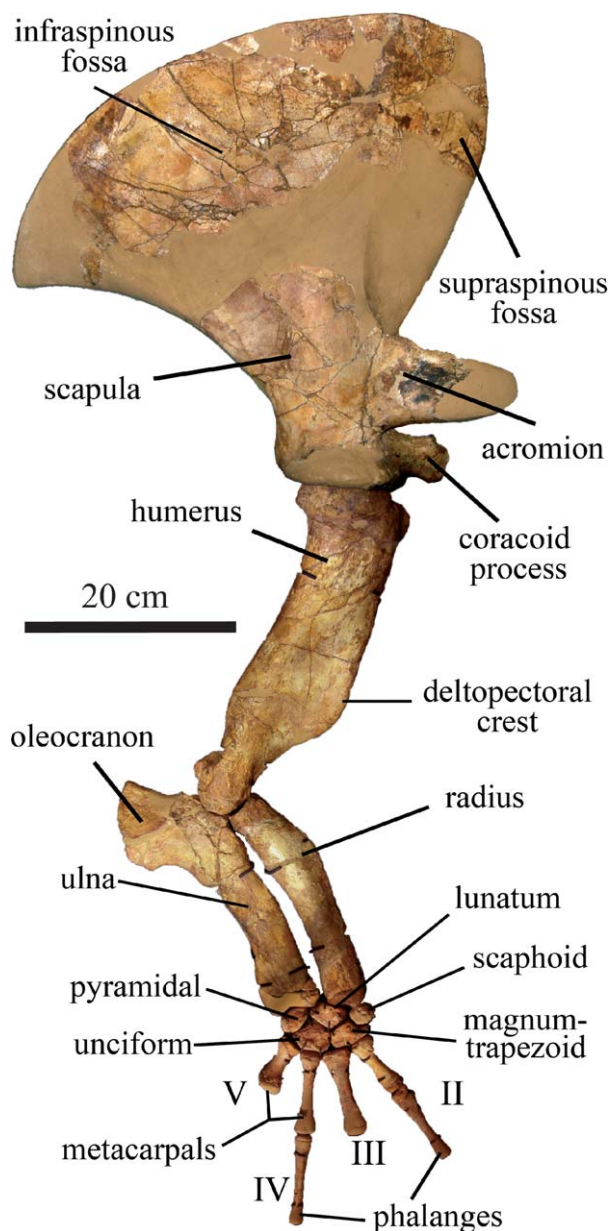


Fig. 6. *Cynthiacetus peruvianus* nov. sp. (holotype MNHN.F.PRU 10). Lateral view of the right forelimb.

Fig. 6. *Cynthiacetus peruvianus* nov. sp. (holotype MNHN.F.PRU 10). Vue latérale du membre antérieur droit.

Chrysocetus is the closer taxon to Neoceti (Uhen, 2004; Uhen and Gingerich, 2001).

As a matter of fact, the basilosaurid skull results to be very constant in all genera of the family and the differences observed on the basicranium appear to be the result of the ontogenetic stage of the specimens compared. The main differences between basilosaurids are observed on the postcranial skeleton. Nevertheless, this preliminary study must be complemented with the construction of a larger matrix including more cranial and postcranial characters. The construction of another matrix based on single

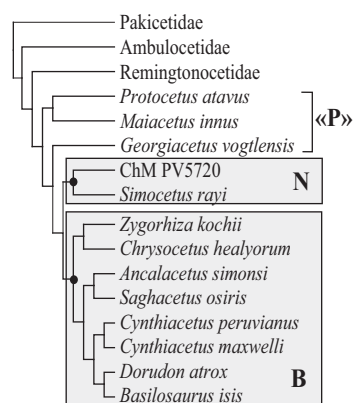


Fig. 7. Consensus tree showing the phylogenetic relationships of *Cynthiacetus* within Basilosauridae. B. Basilosauridae; N. Neoceti; "P": "Protocetidae".

Fig. 7. Arbre consensus montrant les relations phylogénétiques de *Cynthiacetus* au sein des basilosauridés. B. Basilosauridae; N. Neoceti; «P»: «Protocetidae».

specimens instead of taxa will increase the reliability of this study and will reduce the probability of misinterpretations due to polymorphism (in preparation).

Acknowledgements

Special acknowledgements to D. Bohaska, P. Gingerich, G. Gunnell, J. Geisler, G. Phillips and A. Sanders for allowing us the access to the archaeocetes and early neocetes collections under their care. The specimen studied (MNHN.F.PRU 10) was collected with funds of the Institut Français d'études Andines (Lima, Peru) and prepared at the Muséum national d'Histoire naturelle (Paris, France). Photos in Figs. 1, 2 and 5 were realized by P. Loubry and C. Lemzaouda.

Appendix A. Supplementary data

Supplementary data associated with this article can be found, in the online version, at [doi:10.1016/j.crpv.2011.03.006](https://doi.org/10.1016/j.crpv.2011.03.006).

References

- Barnes, L., Mitchell, E., 1978. Cetacea. In: Maglio, V.J., Cooke, H.B.S. (Eds.), Evolution of African mammals. Cambridge University Press, pp. 582–602.
- Brisson, M.J., 1762. Regnum Animale in classes IX distributum sine synopsis methodical. Theodorum Haak, Paris.
- Cope, E.D., 1867. An addition to the vertebrate fauna of the Miocene period, with a synopsis of the extinct Cetacea of the United States. Proc. Acad. Nat. Sci. Philadelphia 19 (4), 138–157.
- DeVries, T.J., 1998. Oligocene deposition and Cenozoic sequence boundaries in the Pisco Basin (Peru). J. South Am. Earth Sci. 11 (3), 217–231.
- DeVries, T.J., Narváez, Y., Sanfilippo, A., Malumian, N., Tapia, P., 2006. New Microfossil evidence for a Late Eocene age of the Otuma Formation (Southern Peru). XIII Congreso Peruano de Geología. Resúmenes Extendidos, pp. 615–618.
- Fitzgerald, E., 2009. The morphology and systematics of *Mammalodon colivieri* (Cetacea: Mysticeti), a toothed mysticete from the Oligocene of Australia. Zool. J. Linn. Soc. 158, 367–476.
- Fordyce, R.E., 1985. Late Eocene archaeocete whale (Archaeoceti: Dorudontinae) from Waihao, South Canterbury, New Zealand. N. Z. J. Geol. Geophys. 28, 351–357.
- Fordyce, R.E., de Muizon, C., 2001. Evolutionary history of cetaceans: a review. In: Mazin, J.M., Buffrénil, V. (Eds.), Secondary adaptation of

- tetrapods to life in water. Verlag Dr. Friedrich Pfeil, München, Germany, pp. 169–223.
- Geisler, J.H., Sanders, A.E., 2003. Morphological evidence for the phylogeny of Cetacea. *J. Mamm. Evol.* 10 (1/2), 23–129.
- Geisler, J.H., Sanders, A.E., Luo, Z., 2005. A New Protocetid Whale (Cetacea: Archaeoceti) from the Late Middle Eocene of South Carolina. *Am. Mus. Novit.* 3480, 1–65.
- Gingerich, P.D., 1992. Marine mammals (Cetacea and Sirenia) from the Eocene of Gebel Mokattam and Fayum, Egypt: stratigraphy, age, and paleoenvironments. *Univ. Mich. Pap. Paleont.* 30, 1–84.
- Gingerich, P.D., 2007. *Stromerius nidensis*, New Archaeocete (Mammalia, Cetacea) from the Upper Eocene Qasr El-Sagha Formation, Fayum, Egypt. *Contrib. Mus. Paleontol.* 31 (13), 363–378.
- Gingerich, P.D., 2010. Cetacea. In: Werdelin, L., Sanders, W. (Eds.), *Cenozoic mammals of Africa*. University of California Press, Berkeley, pp. 873–99.
- Gingerich, P.D., Uhen, M.D., 1996. *Ancalocetus simonsi*, a new dorudontine archaeocete (Mammalia Cetacea) from the early Late Eocene of Wadi Hitan, Egypt. *Contrib. Mus. Paleontol.* 29 (13), 359–401.
- Gingerich, P.D., Smith, B.H., Simons, E.L., 1990. Hind limbs of Eocene *Basilosaurus*: evidence of feet in whales. *Science* 249, 154–157.
- Gingerich, P.D., Arif, M., Bhatti, M.A., Anwar, M., Sanders, W.J., 1997. *Basilosaurus drazindai* and *Basiloterus hussaini*, new archaeoceti (Mammalia Cetacea) from the Middle Eocene Drazinda Formation, with a revised interpretation of ages of whale-bearing strata in the Kirthar Group of the Sulaiman Range, Punjab (Pakistan). *Contrib. Mus. Paleontol.* 30 (2), 55–81.
- Goloboff P.A., Farris J.S., Nixon, K.C., 2003. TNT, Tree analysis using new technology. Program and documentation available from the authors, and at www.zmuc.dk/public/phylogeny.
- Kellogg, R., 1936. A Review of the Archaeoceti. *Carnegie Instit. Wash. Publ.* 482, 1–366.
- Köhler, R., Fordyce, R.E., 1997. An archaeocete whale (Cetacea: Archaeoceti) from the Eocene Waihao Greensand, New Zealand. *J. Vert. Paleontol.* 17 (3), 574–583.
- Luo, Z., Gingerich, P.D., 1999. Terrestrial Mesonychia to aquatic Cetacea: transformation of the basicranium and evolution of hearing in whales. *Univ. Mich. Pap. Paleont.* 31, 1–98.
- Marocco, R., de Muizon, C., 1988. Los vertebrados del Neogeno de La Costa Sur del Perú: Ambiente sedimentario y condiciones de fosilización. *Bull. Inst. fr. études andines* 17 (2), 105–117.
- Uhen, M.D., 1998. Middle to Late Eocene Basilosaurines and Dorudontines. In: Thewissen, J.G.M. (Ed.), *The emergence of whales: evolutionary patterns in the origin of Cetacea*. Plenum Press, New York, pp. 29–61.
- Uhen, M.D., 2004. Form, function, and anatomy of *Dorudon atrox* (Mammalia, Cetacea): an archaeocete from the Middle to Late Eocene of Egypt. *Univ. Mich. Pap. Paleont.* 34, 1–222.
- Uhen, M.D., 2005. A new genus and species of archaeocete whale from Mississippi. *Southeastern Geology* 43 (3), 157–172.
- Uhen, M.D., 2008. New Protocetid whale from Alabama and Mississippi, and a new cetacean clade, Pelagiceti. *J. Vert. Paleontol.* 28 (3), 589–593.
- Uhen, M.D., Gingerich, P.D., 2001. New genus of dorudontine archaeocete (Cetacea) from the Middle-to-Late Eocene of South Carolina. *Mar. Mamm. Sci.* 17 (1), 1–34.
- Uhen, M.D., Pyenson, N., DeVries, T., Urbina, M., 2008. The oldest cetaceans from the Southern Hemisphere: new Archaeocetes from the Pisco Basin of southern Peru. *J. Vertebr. Paleontol.* 28 (3), 154A.